IEEE Access
Multidisciplinary | Rapid Review | Open Access Journal

Received 1 January 2023, accepted 16 January 2023, date of publication 23 January 2023, date of current version 26 January 2023.

Digital Object Identifier 10.1109/ACCESS.2023.3238817

RESEARCH ARTICLE

Buckling Strength Investigation for Power Transformer Winding Under Short Circuit Impact Considering Manufacture and Operation

QIANG OU[1], LONGFU LUO[1], (Member, IEEE), YONG LI[1], (Senior Member, IEEE), YING LI[2], AND JINWEN XIANG[1], (Member, IEEE)

[1]College of Electrical and Information Engineering, Hunan University, Changsha, Hunan 410012, China
[2]TBEA Hengyang Transformer Company Ltd., Hengyang, Hunan 421007, China

Corresponding author: Longfu Luo (llf@hnu.edu.cn)

This work was supported by the National Natural Science Foundation of China under Grant 52061130217.

ABSTRACT Power transformers are inevitably subjected to external short circuit impact during their service period. The electromagnetic force generated by the fault current may cause winding destabilization and collapse. The radial buckling of the inner winding accounts for a considerable proportion. Based on the effective contact of the sticks, the traditional analytical methods ignore the manufacturing deviation and operation impact (MDOI) characterized by assembly gaps and insulation shrinkage. To address the limitation of the contact-constrained approach, this paper proposes the equivalent support stiffness (ESS) analytical method. The ESS method can investigate the issues of support weakening and failure, which are affected mainly by assembly gaps and insulation shrinkage. Further, two transformers are implemented in the short-circuit tests to demonstrate the feasibility of the ESS method. Among them, the assembly gaps are investigated by the first and second windings of the newly manufactured transformer, and the influence of insulation shrinkage is researched through a 30-year-old transformer. Furthermore, the application of the ESS method is expressed based on the tests and the simulations. The research presents quantitative references for transformer design and operational reliability assessment. The ESS method can be an improvement and supplement to traditional methods.

INDEX TERMS Power transformer, winding, short circuit, buckling, manufacture, operation.

NOMENCLATURE

A. ABBREVIATIONS

ESS	Equivalent support stiffness.
HV	High-voltage.
LV	Low-voltage.
MDOI	Manufacturing deviation and operation impact.
TV	Tertiary-voltage.

B. SYMBOLS

Name	*Type*	*Unit*
σ_φ	Equivalent hoop stress	MPa
σ_{cr}	Critical hoop stress	MPa
Δx_{act}	Actual compressed size of material	mm
Δx_0	Initial inner gap caused by the MDOI	mm
A_{st}	Stick area subjected to the radial force	mm^2
b_c	Width of the winding copper strand	mm
B_{zsc}	Short-circuit axial leakage flux density	T
E_0	Equivalent elastic modulus	MPa
E_t	Tangent modulus of elasticity	MPa
f_r	Lorentz force in the radial direction	N/mm^3
F_{act}	Compressive force on each stick	N
h_c	Height of the winding conductor	mm
J_{sc}	Short-circuit current density	A/mm^2
K_{eq}	Equivalent stiffness	N/mm
L_0	Total length of internal support.	mm
N_{st}	Number of the sticks	
R_0	Mean radius of the inner winding	mm

The associate editor coordinating the review of this manuscript and approving it for publication was Vitor Monteiro.

W_{id}	Width of the winding	mm
W_{st}	Width of the stick	mm

I. INTRODUCTION

Power transformer is an essential equipment in electric power systems, and transformer damage caused by an external short circuit may affect the power system's reliability [1]. As the electromagnetic force during short circuit impact is much larger than that of rated operation, short-circuit fault should be paid extra attention to [2], [3]. As shown in Fig.1, the radial failure of inner winding is a crucial issue according to the characteristics of the damage phenomena, such as deformation, forced buckling, and free buckling [4].

When a sufficiently electromagnetic force acts on the winding under short circuit conditions, the copper strand conductor will bend, buckle, collapse, or even damage the transformer [5], [6]. The winding strength research methods include theoretical analysis [7], [8], material research [9], [10], fault analysis [11], test investigation [12], [13], and simulation [14], [15]. Simulation calculation by the finite element method (FEM) has increasingly replaced traditional high-cost and highly destructive experimental research with the continuous improvement of simulation technology [16], [17].

For the analysis of winding strength and stability, it is customary to divide it into two dimensions, the axial and radial components [18], [19]. Among them, radial buckling mainly occurs in the inner winding, related to many factors such as wire type, conductor thickness, and stick number [6], [20]. Radial buckling strength should consider both forced buckling and free buckling. Free buckling occurs when a sufficient gap is present between the inner winding [6]. According to the traditional theoretical research method, the internal supports are equivalent to contact constraints, which do not consider the manufacturing deviation and operation impact (MDOI) [7]. The traditional research method is based on valid support and discusses the influence of winding radius, conductor size, and stick number on the radial failure of the inner winding. However, this judgment method based on sufficient support cannot consider the impact of assembly gap and insulation shrinkage [21]. Transformer manufacturing deviation and winding insulation shrinkage are inevitable in engineering. As a result, it isn't easy to accurately evaluate the mechanical properties of transformer windings based on the fully supported method. Thus, due to the need for more consideration of MDOI, transformer damage during operation and grid breakdown accidents often occur. Unfortunately, the winding radial buckling research considering the influence of MDOI has yet to be described.

To address the above deviation and aging issue, this article proposes the equivalent support stiffness (ESS) method to investigate the radial buckling of inner winding. Further, the effects of support, including the quantity, stiffness, and defect, are simulated by the finite element method (FEM)

FIGURE 1. Typical phenomena of radial buckling failure.

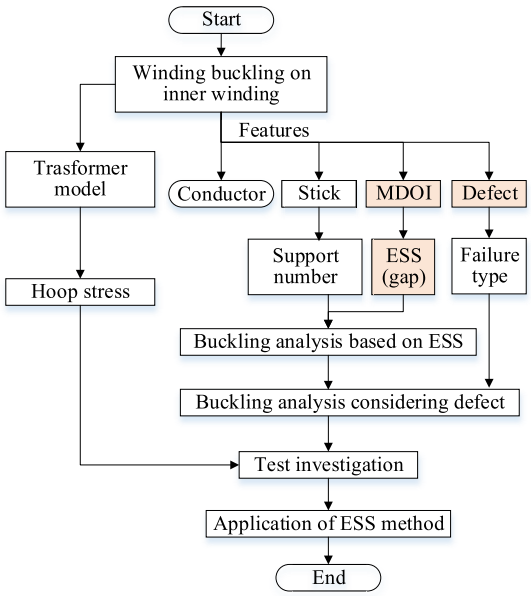

FIGURE 2. Flow chart of ESS method.

based on the ESS method. As the ESS method can consider the influence of MDOI, the results are more accurate when evaluating the winding buckling strength.

The expensive cost and high destructiveness of the transformer short-circuit test determine that the research work in this field is mainly based on materials and models [22]. However, these models cannot reproduce the gaps during manufacturing [23], [24], [25]. To address the issue, two real transformers have been implemented in short-circuit tests to investigate the feasibility of the ESS method. Specifically, one 50MVA/110kV three-phase three-winding transformer is newly designed, and the other is a 30-year-old 150MVA/220kV transformer.

The structure of this paper is organized as shown in Fig.2. Section II proposes the ESS analytical method to investigate the radial buckling strength. Then, the vital characteristic quantities which affect the critical hoop stress are described theoretically, including the conductor, stick, MDOI, and defect. Based on the ESS method, Section III investigates the buckling strength when the defect is ignored and considered, respectively. The short-circuit tests of two actual transformers are implemented in Section IV to demonstrate the ESS method. Further, the application of the ESS method is analyzed based on the tests and the simulations. Finally, the

conclusion and further research plan are expressed in the last section.

II. WINDING RADIAL BUCKLING

A. HOOP STRESS AND BUCKLING STRENGTH

As mentioned above, the transformer windings are subjected to a much larger electromagnetic force under short-circuit conditions than the rated operating conditions. As the difference along each disk of the windings is small in the circumferential direction, a two-dimensional axisymmetric field can generally meet the accuracy requirements for calculating radial force. The hoop stress can be obtained according to the calculated Lorentz force estimated by FEM under shot-circuit impact:

$$\sigma_\varphi = R_0 \cdot f_r = R_0 \cdot J_{sc} \cdot B_{zsc} \tag{1}$$

where σ_φ is the equivalent hoop stress, R_0 is the mean radius of the winding, f_r is the Lorentz force volume density in the radial direction, J_{SC} is the short-circuit current density, and B_{zsc} is the average axial leakage flux density under the short-circuit condition.

When solving the leakage flux distribution of transformer windings, the static field can meet the requirement of solving accuracy. Meanwhile, the ampere-turn method refers to the calculation of loading the rated current on the primary side and the secondary side, respectively. As the influence of excitation reactance is not considered, this method is widely utilized in traditional theoretical calculation and simulation calculation with high computational efficiency. The governing equation of the magnetic field for a transformer can be expressed as follows [4]:

$$\nabla^2 \mathrm{A} = \mu \mathrm{J} \tag{2}$$

where **A** is the magnetic vector potential, μ is the magnetic permeability, and **J** is the current density, denoting short-circuit current.

Based on the steady-state solution method, the leakage flux density distribution and the Lorentz force can be simplified as follows:

$$\begin{cases} B = \nabla \times A \\ \mathrm{f} = \mathrm{J} \times \mathrm{B} \end{cases} \tag{3}$$

where **B** is the leakage flux density, and **f** is the Lorentz force volume density.

Then critical hoop compressive stresses of inner windings are expressed as follows based on IEC60076.5–2006 [5]:

$$\sigma_{cr} = K_s \cdot \sigma_{0.2} \tag{4}$$

where σ_{cr} is the critical hoop stress, also known as buckling stress, $\sigma_{0.2}$ is the proof stress of conductor material, and K_S is the coefficient that depends on the wire type. K_S should be taken as 0.6 when using resin-bonded strands and CTCs wire. In other conditions, K_S should be equal to 0.35.

From (4), the hoop stress generally reaches the buckling stress before the proof value of the material. Thus, the radial buckling analysis is as vital as the hoop stress calculation. Radial buckling stress can be simplified as follows based on the arch stability analytical method [4]:

$$\sigma_{cr} = \frac{E_t}{12}\left(\frac{b_c}{R_0}\right)^2 \left[\left(\frac{\pi}{\alpha}\right)^2 - 1\right] \tag{5}$$

where E_t is the tangent modulus of elasticity, b_c is the width of the winding copper strand, π/α reflects the characteristic of buckling mode, and α is the angle between the radial adjacent supports.

The buckling stress is related to the material, the width of the copper strand, and the winding mean radius. Meanwhile, the buckling mode and critical stress change with valid support quantity and support stiffness. As the influence of copper wire has been studied in other literature, this paper will focus on the effect of internal support on radial stability.

B. STICK SUPPORT STIFFNESS

When investigating the sticks' compressive deformation, the self-supporting effect of the conductor on the radial direction is ignored. Thus, the compressive force on each stick in the radial direction can be approximately given by:

$$F_{act} = \frac{2\pi \cdot f_r \cdot W_{id} \cdot h_c \cdot R_0}{N_{st}} \tag{6}$$

where F_{act} is the compressive force on each stick, W_{id} is the width of the winding, h_c is the height of the winding conductor, and N_{st} is the number of sticks.

The radial support inside the winding is influenced by insulation cylinders, sticks, and core, which cannot be simply equivalent to either valid or invalid support. More cases may be between free buckling and forced buckling. When the radial force is transmitted to the internal support structure, the surface subjected to the force is the stick area. Then, the comprehensive equivalent elastic modulus of different materials inside the winding can be calculated as [4]:

$$E_0 = \frac{L_W + L_S + L_C}{L_W/E_W + L_S/E_S + L_C/E_C} \tag{7}$$

where L_W, L_S, and L_C are the length of the winding portion, stick portion, and core portion, respectively, E_W, E_S, and E_C are Young's modulus of the winding portion, stick portion, and core portion, and E_0 is the equivalent elastic modulus.

The stick's inner surface inside the winding is set as the equivalent stiffness boundary constraint during the calculation. Then, the stiffness coefficient of the support structure can be expressed as:

$$K_{eq0} = \frac{E_0 \cdot A_{st}}{L_0} = \frac{E_0 \cdot W_{st} \cdot h_c}{L_0} \tag{8}$$

where K_{eq0} is the equivalent stiffness when ignoring the effect of MDOI, A_{st} is the stick area subjected to the radial force, W_{st} is the stick width, and L_0 is the total length of the internal support structure. It should be noted that the above formula is only a theoretical value when ignoring the gap in the winding assembly process and the shrinkage of the insulation material. Further, the winding is not fully supported by sticks and core,

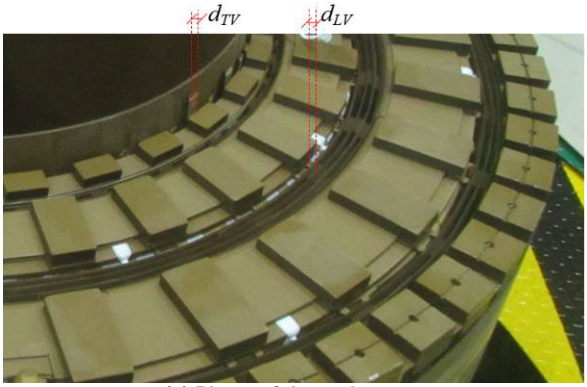

(a) Photo of the active part

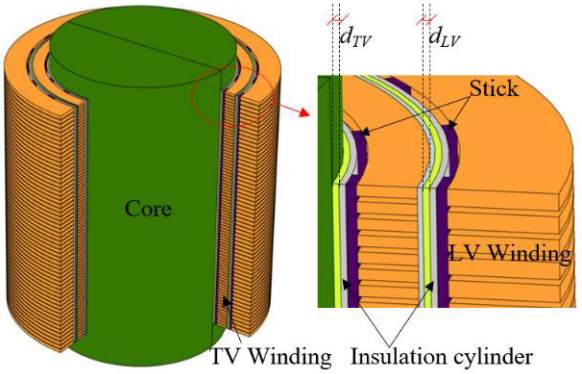

(b) Schematic diagram

FIGURE 3. Support structure of the winding.

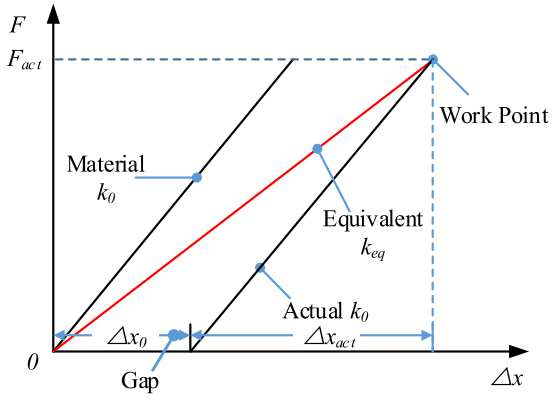

FIGURE 4. Calculation principle of the ESS method.

and K_{eq} will be smaller than the theoretically calculated value based on (8) when considering the gaps.

C. EQUIVALENT SUPPORT STIFFNESS METHOD

There are inevitable effects of the MDOI during a transformer service period, such as assembly gaps and insulation shrinkage. This paper proposes the ESS method to address the limitation of traditional research methods of direct contact constraint. The radial buckling strength can be calculated by defining the ESS of internal support and assuming support failures.

TABLE 1. Winding Parameters.

Item	New TV	New LV	Old TV	Old LV
Rated power (MVA)	50	50	75	150
Rated voltage (kV)	38.5	10.5	11	121
Impedance (%)	18.56	11.09	24.34	14.2
Disk number	79	58	102	86
Electrical turns	79	167	51	324
Inner radius (mm)	363	430	477	562
Radial build (mm)	45	82.5	37	113.5
Copper strand type	Flat conductor			
Conductor thickness (mm)	1.52	2.9	2.5	2.5
Conductor width (mm)	8.0	12.3	11.2	12.5
Proof stress (MPa)	140	140	90	90
Sticks quantity	20	20	28	28

It is considered that newly manufactured transformers are in a defect-free state, while most of the old transformers have local flaws. Furthermore, the ESS research method is based on the actual engineering situation with specific assembly gaps, as shown in Fig.3. The closer the windings are to the core, the smaller the assembly gap will be, and the gap will add up after multiple layers. The schematic and calculation of the ESS method are described as follows.

As shown in Fig.3, the assembly gaps d_{TV} and d_{LV} are the winding unavoidable assembly gaps expressed as Δx_0. When the disk is compressed by uniform force, there is no adequate support during this gap. The winding will be supported after the displacement reaches Δx_0. As the elastic modulus of the core and copper is much larger than that of the insulation material in the support structure, the compression of the core and copper can be ignored.

Fig.4 shows the calculation principle of the ESS analytical method. The deformation of the main insulation, including the stick and the insulation cylinder, is considered independently. According to the curve relationship, the value of the ESS can be calculated as follows:

$$K_{eq} = \frac{F_{act}}{\Delta x_{act} + \Delta x_0} = \frac{\Delta x_{act} \cdot K_{eq0}}{\Delta x_{act} + \Delta x_0} \tag{9}$$

where K_{eq} is the ESS of support material proposed in this paper to investigate the MDOI, Δx_{act} is the actual compressed size, and Δx_0 is the winding initial inner gap caused by the MDOI.

The compression deformation of the support structure can be obtained at the work point when assuming no compression deformation of the core and inner copper structure. Then, combining (1), (6), and (8) with the stress-strain relationship, approximately taking a linear segment, the compression deformation can be expressed as follows:

$$\Delta x_{act} = \frac{F_{act}}{E_0 \cdot A_{st}} L_0 = \frac{2\pi \cdot \sigma_\varphi \cdot W_{id} \cdot L_0}{E_0 \cdot W_{st} \cdot N_{st}} \tag{10}$$

III. RADIAL BUCKLING ANALYSIS

A. WINDING RADIAL FORCE

Two transformers are implemented in the short-circuit tests to investigate the effect of radial supports on the winding

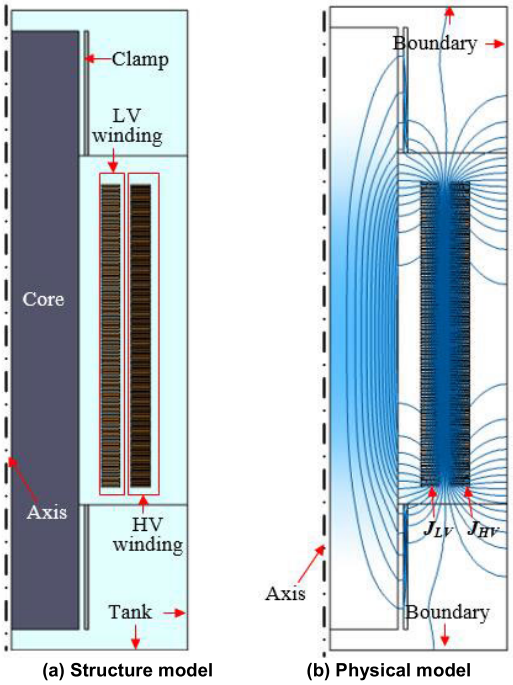

FIGURE 5. FEM model diagram.

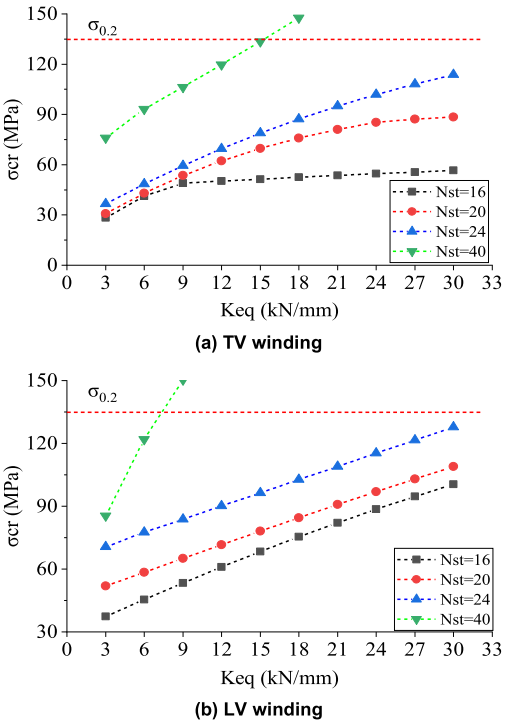

FIGURE 6. Buckling stress when ignoring failure.

buckling. Specifically, the difference between the first and second windings is compared by a newly manufactured transformer with the power of 50MVA, and the influence of insulation shrinkage is investigated through a 30-year-old transformer with the power of 150MVA. Detailed parameters of inner windings are given in Table 1.

Based on the FEM, the two-dimensional axisymmetric and the three-dimensional field are utilized to calculate the leakage flux and each disk's electromagnetic force by the finite element program COMSOL Multiphysics 6.0. The HV-LV condition is an example to present the model, boundary conditions, and results.

Fig.5a shows the geometric model, which is described by the outside area of the core window. The primary material consists of a high-magnetic-permeability core, low-magnetic-permeability clamps, and non-magnetic-permeability copper. In Fig.5b, the current is applied to the winding position, and the simulated leakage flux distribution is shown. It can be seen that the axial leakage flux in the middle of the windings is significantly larger than that at both ends.

B. BUCKLING ANALYSIS BASED ON ESS

The radial buckling is simulated by changing the inner winding support's ESS values to investigate the influence of the assembly gap and the number of adequate supports. Based on (9), the maximum ESS value of the new LV winding can be approximately calculated as follows:

$$K_{eq\,\max} = \frac{8 \times 19 \times 12.3}{40 + 0} = 46.7\text{kN/mm} \tag{11}$$

Meanwhile, the minimum ESS value of the new LV winding can be expressed as follows:

$$K_{eq\,\min} = \frac{0.2913 \times 46.7}{0.2913 + 5} = 2.6\text{kN/mm} \tag{12}$$

where E_0 is the elastic modulus of the material, 8GPa [15], L_0 is taken as 40mm, A_{st} is taken as 19mm×12.3mm, Δx_0 is assumed as 5mm caused by the MDOI according to process requirement, and Δx_{act} is the actual insulation compression calculated by (10) under short-circuit conditions, 0.291mm.

The ESS value is taken from 3 to 30 kN/mm with the step 3kN/mm to investigate the gap effects caused by the assembly process and insulation shrinkage. The buckling stresses of TV and LV winding are calculated by finite element simulation under different equivalent stiffness. And the values of TV and LV winding are compared in Fig.6. If the computed value exceeds the proof stress, it should be judged as strength failure first before buckling, and the corresponding buckling forms will not appear in practice.

Compare the difference between TV and LV winding:

(1) The buckling stress on LV is greater than TV winding because the thickness of LV and TV conductor is 2.9mm and 1.52mm, respectively. Therefore, the thickness of the conductor is the crucial factor affecting the buckling strength.

(2) Under the same support quantity and stiffness, the radial buckling stress is positively related to the conductor thickness. The result is consistent with the conclusion in (5).

(3) For the same conductor, the buckling stress increase with the support quantity and stiffness. Therefore, ensuring

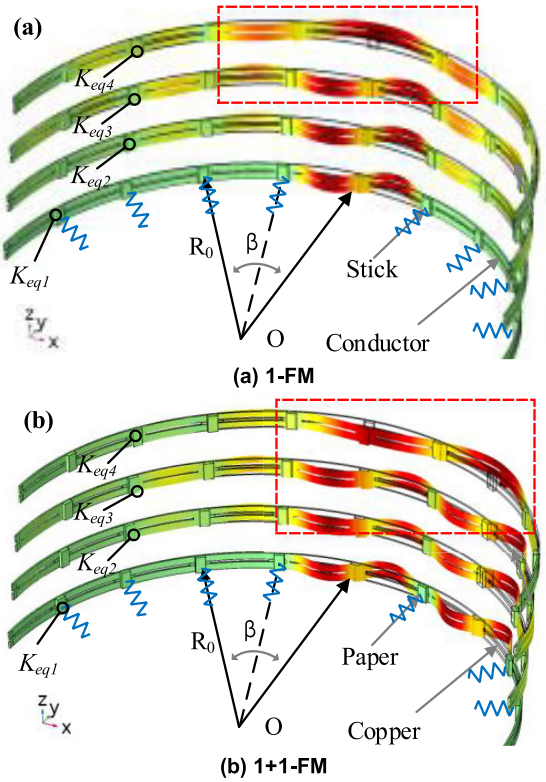

FIGURE 7. Plot of radial buckling modes.

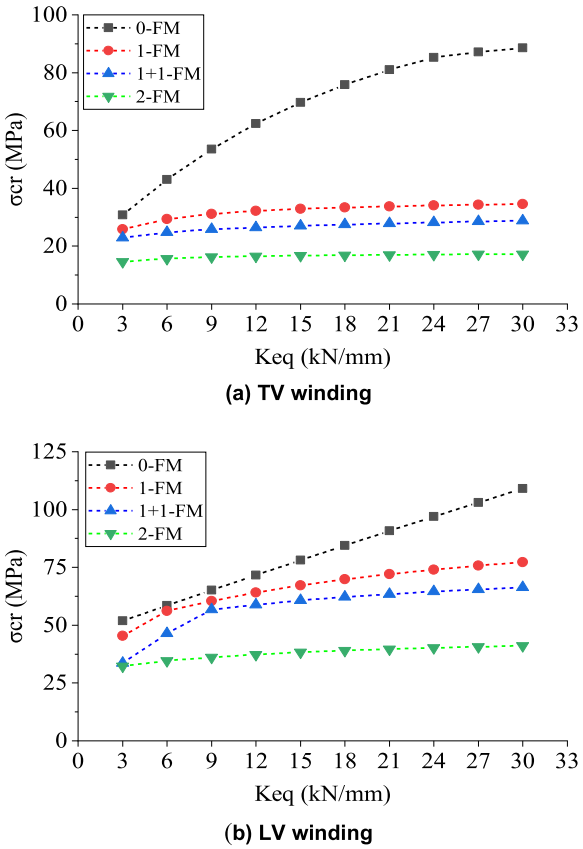

FIGURE 8. Buckling stress considering the failure.

the support stiffness and increasing the stick quantity can improve the winding ability to withstand short circuit.

C. BUCKLING ANALYSIS CONSIDERING DEFECT

It can be observed that the buckling stress correspondingly increases with the stick quantity. However, it does not strictly obey the form of (5) in practice. The buckling stress of TV and LV winding differs between the support stiffness and stick quantity. That means the support stiffness and stick are as crucial as the effect of conductor thickness on the winding radial buckling.

To further investigate the relationship between π/α and the buckling mode, the manufacturing dispersion and defects are simulated by assuming the failure point of the support. Manufacturing dispersion and defects may cause one or more support failures during specific equivalent treatment. Thus, four different equivalent conditions are analyzed by taking the stick quantity 20 as an example. Specifically, there is no defect in the ''No failure'' model (0-FM). The ''One failure'' model (1-FM) simulates the state that there is one defect in the circle. Moreover, the ''Two adjacent failures''(2-FM) model and the ''Two non-adjacent failures'' model (1+1-FM) simulate two support failures, but the missing support points are continuous and non-adjacent, respectively. With the help of COMSOL Multiphysics, The linear buckling study is utilized to estimate the critical load at which a structure becomes unstable. Further, the LV winding radial buckling forms in different failures are shown in Fig.7. Where, K_{eq1}, K_{eq2}, K_{eq3}, and K_{eq4} represent the results of the equivalent stiffness of 3, 12, 21, and 30kN/mm, respectively.

There are apparent differences in the buckling mode of different defect types by comparing Fig.7a and Fig.7b. Further, the buckling stress values of the same defect with different stiffness can be obtained by observing the red dotted lines. It can be noted that the buckling mode will change if the support stiffness is reduced to a particular value. Fig.8 details the buckling stress of TV and LV winding under different support conditions.

The following conclusions are obtained by analyzing the results under different conditions:

(1) The influence of conductor thickness is the greatest when analyzing buckling stress under similar working conditions. The LV value is 68.5% higher than the value of TV winding by taking K_{eq} =3 kN/mm, 0-FM condition as an example. And the LV stress is 123.8% higher than the TV value under K_{eq} =30 kN/mm, 1-FM.

(2) Taking 0-FM as an example, with the support stiffness rising from 3 to 30 kN/mm, the TV and LV winding buckling stresses are increased by 187.5% and 110.2%, respectively.

The buckling stress increases with the support quantity and the ESS. However, when the local support failure range is too extensive in 2-FM, the radial buckling changes are no longer evident with the number and stiffness. Therefore, ensuring the

TABLE 2. Test current and critical stress.

Test number	1	2	3	4	5
Duration (s)	0.236	0.236	0.238	0.249	0.235
Peak current(A)	5557	6675	7602	8611	9675
RMS current (A)	2069	2456	2783	3125	3463
Inductance (mH)	141.5	141.8	141.9	141.9	143.8
Impedance change (%)	-0.20	0.03	0.06	0.10	1.42

TABLE 3. Test current and critical stress.

Item	New TV	New LV	Old TV	Old LV
Peak current (kA)	24451	15516	36576	9675
Buckling stress (MPa)	37.9	40.5	50.5	24.9
Proof stress (MPa)	140	140	90	90
The ratio of stress	27.1%	28.9%	56.1%	27.7%

tightness and uniformity of the winding assembly margin is an effective method to improve winding radial strength.

IV. SHORT-CIRCUIT TEST INVESTIGATION

There are inevitable assembly gaps and manufacturing deviations during the manufacturing process. Meanwhile, the internal support will weaken and might fail with the operating years because of the insulation aging and shrinkage. As the MDOI is objective and unavoidable, the MDOI's impact cannot be ignored. The limitations of the traditional research method based on effective contact can be addressed by the ESS method. In this section, the rationality of the ESS method will be investigated through short-circuit tests. What's more, the regional scope of gap and failure will be scanned.

A. SHORT-CIRCUIT TEST AND DISASSEMBLY

The short-circuit tests of the two transformers have different research focuses. Specifically, the newly manufactured transformer distinguishes the ESS between the first and second windings, and the influence of insulation shrinkage is considered through the old one.

The short-circuit tests aim to determine the critical short-circuit current, buckling stress, and deformation states. Thus, the tests are implemented by gradually increasing the current. The impedance is measured after each test. It is considered that permanent internal deformation has occurred if the change exceeds 1.0% of the IEC60076-5 standard judgment range. Then the short circuit test will be ended. Meanwhile, the short-circuit currents take the maximum current in a set of tests as the critical value when ignoring the test deviation and the cumulative damage. Taking the old LV short-circuit test as an example, the test data is shown in Table 2:

The short-circuit test is performed to apply load on the HV side. The inductance directly measured on the HV side is recorded, and the currents in the table have been converted to the LV side.

Table 3 lists the critical short-circuit currents and the radial critical stresses obtained by secondary FEM simulation based on the critical currents. Since the buckling stress is much smaller than the proof stress, it is necessary to pay attention to the radial buckling strength.

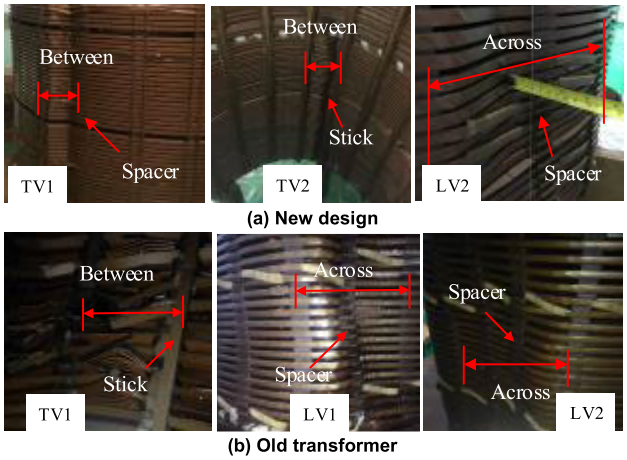

FIGURE 9. Deformation phenomena of inner windings.

TABLE 4. ESS calculation.

Item	New TV	New LV	Old TV	Old LV
L_0 (mm)	18.0	40.0	18	70.0
W_{st} (mm)	19.0	19.0	19	19.0
$\triangle x_{act}$ (mm)	0.0635	0.2913	0.0794	0.4673
K_{eq0}	67.6	46.7	60.7	17
$K_{eq1}(\triangle x_0{=}1)$	4.0	10.5	4.5	5.4
$K_{eq2}(\triangle x_0{=}2)$	2.1	5.9	2.3	3.2
$K_{eq3}(\triangle x_0{=}3)$	1.4	4.1	1.6	2.3
$K_{eq4}(\triangle x_0{=}4)$	1.1	3.2	1.2	1.8
$K_{eq5}(\triangle x_0{=}5)$	0.9	2.6	0.9	1.5
$K_{eq6}(\triangle x_0{=}6)$	0.7	2.2	0.8	1.2
$K_{eq7}(\triangle x_0{=}7)$	0.6	1.9	0.7	1.1
$K_{eq8}(\triangle x_0{=}8)$	0.5	1.6	0.6	0.9

The equivalent support stiffness *Keq* is in kN/mm.

After all the tests, the units are transported back and disassembled to observe the buckling mode. Both the new design and the old transformer are three-phase three-winding transformers, each including three TV windings and three LV windings. Fig.9 shows pictures of inner windings with typical radial failures.

Two important conclusions can be obtained based on the disassembly phenomena:

(1) There are better supports on new TV winding, and the damages tend to be forced buckling with the deformation between the adjacent sticks. Therefore, it should be equivalent to a strong support relationship.

(2) The LV winding of the old transformer operating for approximately 30 years, is seriously deformed, crossing the adjacent sticks. And the radial buckling mode is no longer half the number of sticks. Accordingly, this support can be equivalent to a weak support relationship.

The TV winding is situated close to the core, and there is relatively better internal support than LV winding which has more assembly gaps. Meanwhile, the support weakening and failure are affected by insulation aging and shrinkage, and the

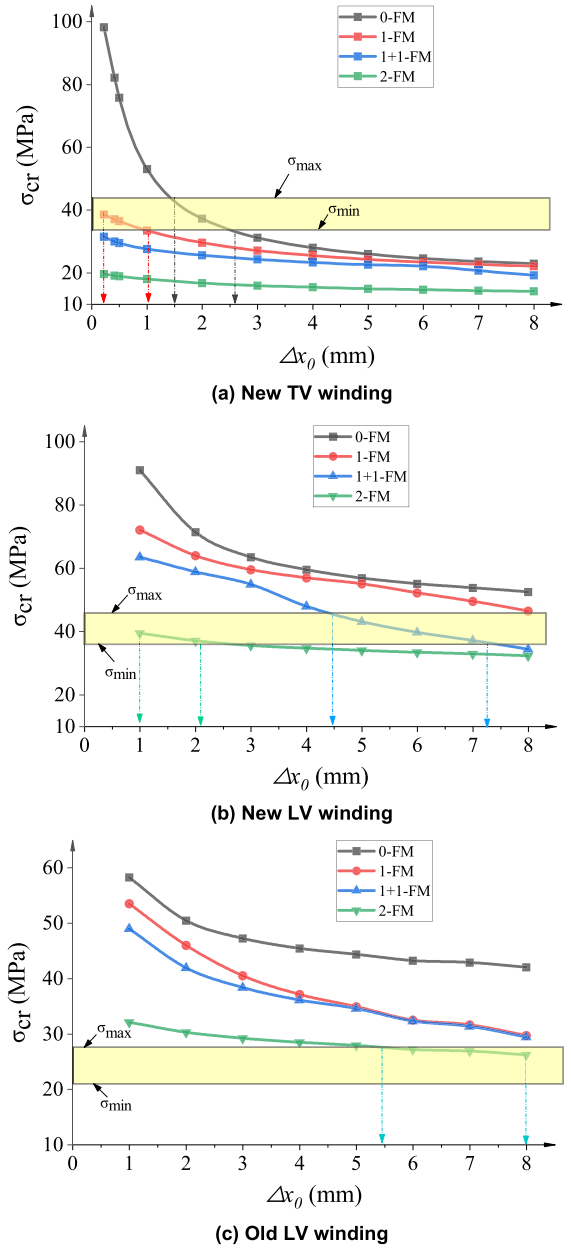

FIGURE 10. Curve of buckling stress-winding gap.

old LV winding buckling mode is significantly reduced with operating years. In conclusion, the MDOI cannot be ignored in engineering.

B. APPLICATION OF THE ESS METHOD

The influence of support conditions and operation age on radial buckling has been investigated through FEM simulation and short-circuit tests. Based on the proposed ESS method, the theoretical ESS value of each winding is calculated by (9), and the calculation results are listed in Table 4.

For more in-depth research and application, the buckling finite element simulation can obtain the adaptation domain of the ESS method and MDOI. The ESS values are calculated by

TABLE 5. Relationship between buckling stress and assembly gap.

Δx_0	New TV		New LV	
	σ_{cr} (MPa)	$\Delta\sigma_{cr}$ (%)	σ_{cr} (MPa)	$\Delta\sigma_{cr}$ (%)
1	53.05	/	90.94	/
2	37.29	-29.72	71.35	-21.55
3	31.11	-41.35	63.48	-30.20
4	27.92	-47.37	59.50	-34.57
5	25.92	-51.14	56.85	-37.49
6	24.57	-53.68	55.07	-39.44
7	23.60	-55.51	53.74	-40.91
8	22.82	-56.98	52.41	-42.37

TABLE 6. Relationship between buckling stress and support failure.

Failure Model	Old TV		Old LV	
	σ_{cr} (MPa)	$\Delta\sigma_{cr}$ (%)	σ_{cr} (MPa)	$\Delta\sigma_{cr}$ (%)
0-FM	37.29	/	44.35	/
1-FM	29.57	-20.70	34.88	-21.35
1+1-FM	25.54	-31.50	34.57	-22.05
2-FM	16.73	-55.13	27.87	-37.17

scanning the initial gaps from 1mm to 8mm in Table 4, then the curves of buckling stress with the initial gaps are plotted in Fig.10.

According to engineering practice, the deviations of manufacture, calculation, and short-circuit tests are assumed as 3%, 3%, and 10%, respectively. Then, the 100% ±10.9% value can be taken as a credible contour area. As shown in Fig.10, the yellow areas are the confidence range considering the ESS and defect.

The old transformer is more prone to local defects as they are more seriously affected by MDOI. Moreover, the assembly gap of LV winding is bigger than that of TV winding which is closer to the core. Therefore, when taking the value, the "0-FM" or "1-FM" should be the focus in Fig.10a and Fig.10b. Correspondingly, the "1+1-FM" or "2-FM" in Fig.10c is more prone to occur.

Through observing and approximate interpolation calculation, the states of the three windings can be obtained as follows:

(1) The state of new TV winding may be the "0-FM" with a value of Δx_0 1.70 ∼ 2.56mm or the "1-FM" with a value of Δx_0 less than 0.94mm.

(2) The new LV winding may occur the "1+1-FM" with the value of Δx_0 4.62 ∼ 7.36mm.

(3) The old LV winding should take the "2-FM" with a value of Δx_0 more than 5.37mm.

The initial gap and the credible failure area are obtained using a certain deviation range. Then, the values can be utilized as a reference for transformer design and operational reliability assessment. In addition, transformer failure points will increase with operating age because of plastic deformation. Furthermore, the initial gap range of the LV winding is more significant than that of the TV winding.

C. PERFORMANCE LOSS CAUSED BY MDOI

The ESS method can evaluate the influence of the assembly gap for the newly manufactured transformer winding on the mechanical properties. Table 5 data can be a reference:

The results show that the critical hoop stress value of both TV and LV winding will decrease rapidly with the increase of assembly gap, and the proportion can reach 20%∼50%. Improving manufacturing control ability and reducing assembly gap is superior to reducing current density or increasing conductor thickness in cost.

Based on another aspect of this paper, performance evaluations of operating transformers that consider support failures are also very valuable. The reason for this failure may be from insulation aging, short circuit impact compression, and stick shift. The influence data are shown in Table 6.

Once more than one support failure occurs in operation, the winding ability to withstand short circuits will also be reduced by more than 20%. When considering manufacture and operation, the actual buckling strength of power transformer winding is lower than that under the ideal adequate support conditions.

The strength checks ignoring the MDOI influence cannot accurately characterize the mechanical properties of the transformer winding. More importantly, this strength weakening may cause changes in transformer operating parameters, such as impedance and noise, thus endangering the safe operation of the grid. Therefore, the influence of MDOI is very significant when investigating the winding strength under short circuit impact.

V. CONCLUSION

The support boundaries, including the support stiffness and failure, significantly affect the radial buckling strength of power transformer winding. By proposing the ESS method, this paper investigates the buckling strength considering the MDOI characterized by assembly gaps and insulation shrinkage. The feasibility of the ESS method has been demonstrated by two short-circuit tests. One is a new 110kV design, and another is a 30-year-old 220kV transformer.

When applying the ESS method, the manufacturing deviation values of TV and LV winding can be taken as 1mm and 5mm, respectively, based on the test samples in this paper. Further, support failures can simulate the support weakening and defects caused by insulation shrinkage. The research presents quantitative references for transformer design and operational reliability assessment.

As the limited sample short-circuit tests cannot sufficiently characterize the short-circuit characteristics of all transformers, more tests would be performed for further research in the future. By improving the ESS method proposed in this paper, the relationship between transformer radial buckling strength and MDOI can be obtained more accurately and quickly.

ACKNOWLEDGMENT

CIGRE is represented by Anders Lindroth.

REFERENCES

[1] A. I. Lur'e, "Transformer connection under no-load and short-circuit events," *Russian Electr. Eng.*, vol. 79, no. 2, pp. 57–70, Feb. 2008.

[2] *IEEE Guide for Establishing Short-Circuit Withstand Capabilities of Liquid-Filled Power Transformers, Regulators, and Reactors*, IEEE Standard C57.164^{TM}-2021, 2021.

[3] *IEEE Standard Test Code for Liquid-Immersed Distribution, Power, and Regulating Transformers*, IEEE Standard C57.12.90-2015, pp. 67–75, 2015.

[4] H. J. Zhang, S. H. Wang, and S. Wang, "Cumulative deformation analysis of transformer winding under short-circuit fault using 3-D FEM," in *Proc. IEEE Int. Conf. Appl. Supercond. Electromagn. Devices (ASEMD)*, Nov. 2015, pp. 370–371.

[5] *Power Transformer—Parts5: Ability to Withstand Short Circuit*, Standard IEC 60076-5, 2006.

[6] I. Kumar and A. Bakshi, "Effects of axial sticks and proof stress of conductor material on the buckling strength of transformer inner winding," *IEEE Trans. Power Del.*, vol. 37, no. 6, pp. 5465–5468, Dec. 2022.

[7] M. R. D. Vecchio, B. Poulin, P. T. Feghali, D. M. Shah, and R. Ahuja, *Transformer Design Principles*, 3rd ed. London, U.K.: CRC Press, 2018, pp. 260–279.

[8] A. Lindroth, "The short-circuit performance of power transformers," CIGRE, Paris, France, Tech. Rep. 209, 2002.

[9] Y. Zhao, W. Chen, M. Jin, T. Wen, J. Xue, Q. Zhang, and M. Chen, "Short-circuit electromagnetic force distribution characteristics in transformer winding transposition structures," *IEEE Trans. Magn.*, vol. 56, no. 12, pp. 1–8, Dec. 2020.

[10] S. Zhang, Z. Wang, Z. Xu, and N. Chai, "A study on bending properties of CTCs in hot state," in *Proc. Int. Conf. Power Syst. Technol. (POWERCON)*, Dec. 2021, pp. 2241–2245.

[11] G. Venkateswarlu, Y. Agarwal, and M. S. Takkher, "Significance of tank current measurement during short circuit testing of power transformer," in *Proc. Int. Conf. High Voltage Eng. Technol. (ICHVET)*, Feb. 2019, pp. 1–5.

[12] Y. Shi, S. Ji, F. Zhang, F. Ren, L. Zhu, and L. Lv, "Multi-frequency acoustic signal under short-circuit transient and its application on the condition monitoring of transformer winding," *IEEE Trans. Power Del.*, vol. 34, no. 4, pp. 1666–1673, Aug. 2019.

[13] H.-M. Ahn, Y.-H. Oh, J.-K. Kim, J.-S. Song, and S.-C. Hahn, "Experimental verification and finite element analysis of short-circuit electromagnetic force for dry-type transformer," *IEEE Trans. Magn.*, vol. 48, no. 2, pp. 819–822, Feb. 2012.

[14] S. Wang, S. Wang, H. Li, D. Yuan, and S. Wang, "Mechanical characteristics analysis of defective transformer windings under short-circuit fault using 3-D FEM," in *Proc. 20th Int. Conf. Electr. Mach. Syst. (ICEMS)*, Aug. 2017, pp. 1–4.

[15] H. Zhang, B. Yang, W. Xu, S. Wang, G. Wang, Y. Huangfu, and J. Zhang, "Dynamic deformation analysis of power transformer windings in short-circuit fault by FEM," *IEEE Trans. Appl. Supercond.*, vol. 24, no. 3, pp. 1–4, Jun. 2014.

[16] B. Bosnjak, G. Leber, and H. Landes, "Coupled 3D transient magneto-mechanical FEM simulation of a short circuit test on a mock-up of a 570 MVA transformer unit," *Proc. Eng.*, vol. 202, pp. 224–230, Jan. 2017.

[17] C. Zhang, W. Ge, Y. Xie, and Y. Li, "Comprehensive analysis of winding electromagnetic force and deformation during no-load closing and short-circuiting of power transformers," *IEEE Access*, vol. 9, pp. 73335–73345, 2021.

[18] M. Jin, W. Chen, Y. Zhao, T. Wen, J. Wu, X. Wu, and Q. Zhang, "Coupled magnetic-structural modeling of power transformer for axial vibration analysis under short-circuit condition," *IEEE Trans. Magn.*, vol. 58, no. 7, pp. 1–9, Jul. 2022.

[19] A. Moradnouri, M. Vakilian, A. Hekmati, and M. Fardmanesh, "Optimal design of flux diverter using genetic algorithm for axial short circuit force reduction in HTS transformers," *IEEE Trans. Appl. Supercond.*, vol. 30, no. 1, pp. 1–8, Jan. 2020.

[20] A. Bakshi, "Effect of width of axial supporting spacers on the buckling strength of transformer inner winding," *IEEE Trans. Power Del.*, vol. 34, no. 6, pp. 2278–2280, Dec. 2019.

[21] A. Bakshi and S. V. Kulkarni, "Analysis of buckling strength of inner windings in transformers under radial short-circuit forces," *IEEE Trans. Power Del.*, vol. 29, no. 1, pp. 241–245, Feb. 2014.

[22] S. Acharya and P. C. Tapre, "Life assessment of transformer using thermal models," in *Proc. Int. Conf. Energy, Commun., Data Anal. Soft Comput. (ICECDS)*, Aug. 2017, pp. 3515–3520.

[23] C. Yan, Y. Wei, C. Xu, and B. Zhang, "Experimental verification and electromagnetic–mechanics–acoustic field coupling analysis of transformer pressure relief valve malfunctions due to external short-circuit faults," *IEEE Trans. Magn.*, vol. 55, no. 6, pp. 1–4, Jun. 2019.

[24] D. D. Shipp, T. J. Dionise, V. Lorch, and B. G. MacFarlane, "Transformer failure due to circuit-breaker-induced switching transients," *IEEE Trans. Ind. Appl.*, vol. 47, no. 2, pp. 707–718, Mar. 2011.
[25] D. Geissler and T. Leibfried, "Mechanical breakdown of aged insulating paper around continuously transposed conductors for power transformers under the influence of short-circuit forces—Analysis by numerical simulations," in *Proc. IEEE Electr. Insul. Conf. (EIC)*, Aug. 2015, pp. 401–406.

QIANG OU was born in Sichuan, China, in 1983. He received the B.S. degree from the College of Electrical Engineering, Taiyuan University of Technology, Taiyuan, China, in 2006, and the M.S. degree from the College of Electrical Engineering, Xi'an Jiaotong University, Xi'an, China, in 2012. He is currently pursuing the Ph.D. degree in electrical engineering with the College of Electrical and Information Engineering, Hunan University.

Since 2018, he has been a Senior Engineer of electrical engineering. His current research interests include the design and performance optimization of HV electromagnetic equipment, especially the theoretical study and engineering application in the electromagnetic field and mechanical strength field of power transformers.

LONGFU LUO (Member, IEEE) was born in Hunan, China, in 1962. He received the B.Sc., M.Sc., and Ph.D. degrees from the College of Electrical and Information Engineering, Hunan University, Changsha, China, in 1983, 1991, and 2001, respectively.

From 2001 to 2002, he was a Senior Visiting Scholar at the University of Regina, Regina, SK, Canada. He is currently a Full Professor of electrical engineering with the College of Electrical and Information Engineering, Hunan University. His current research interests include the design and optimization of modern electrical equipment, the development of new converter transformer, and the study of corresponding new HVDC theories.

YONG LI (Senior Member, IEEE) was born in Henan, China, in 1982. He received the B.Sc. and Ph.D. degrees from the College of Electrical and Information Engineering, Hunan University, Changsha, China, in 2004 and 2011, respectively, and the second Ph.D. degree from TU Dortmund University, Dortmund, Germany, in 2012. Since 2009, he has been a Research Associate with the Institute of Energy Systems, Energy Efficiency, and Energy Economics, TU Dortmund University. After then, he was a Research Fellow with The University of Queensland, Brisbane, QLD, Australia. Since 2014, he has been a Full Professor of electrical engineering with Hunan University. His current research interests include power system stability analysis and control, ac–dc energy conversion systems and equipment, analysis and control of power quality, and HVDC and FACTS technologies.

YING LI was born in Liaoning, China, in 1970. She received the B.S. degree in electrical engineering from the Shenyang University of Technology, Shenyang, China, in 1992, and the M.S. degree in electrical engineering from Hunan University, Changsha, China, in 2013. From 1992 to 2002, she was a Senior Engineer at the New Product Development Department, Shenyang Transformer Company Ltd. She has been a Technical Expert with the Technology Management Department, TBEA Hengyang Transformer Company Ltd., since 2002. Her research interests include electromagnetic fields, oil flow temperature rise, and mechanical strength of UHV transformers.

JINWEN XIANG (Member, IEEE) was born in Yiyang, China, in 1991. He received the B.S. and M.S. degrees in electrical engineering from Hunan University, Changsha, China, in 2014 and 2017, respectively, where he is currently pursuing the Ph.D. degree in electrical engineering with the College of Electrical and Information Engineering. His current research interests include power quality control, power electronics and drives for transportation, and renewable energy application.